water

Article

Weathering Intensity Response to Climate Change on Decadal Scales: A Record of Rb/Sr Ratios from Chaonaqiu Lake Sediments, Western Chinese Loess Plateau

Lipeng Liu [1], Keke Yu [1,2,3,*], Aizhen Li [1], Chao Zhang [1], Le Wang [3], Xingxing Liu [3] and Jianghu Lan [3,4,*]

1 College of Geography and Environment, Baoji University of Arts and Sciences, Baoji 721013, China; bwlllp1996@163.com (L.L.)
2 Key Laboratory of Disaster Monitoring and Mechanism Simulation of Shaanxi Province, Baoji 721013, China
3 State Key Laboratory of Loess and Quaternary Geology, Institute of Earth Environment, Chinese Academy of Sciences, Xi'an 710061, China
4 Laoshan Laboratory, Qingdao 266061, China
* Correspondence: yukezan2005@163.com (K.Y.); lanjh@ieecas.cn or lanjh115@163.com (J.L.); Tel./Fax: +86-29-6233-6295 (J.L.)

Abstract: The Rb/Sr ratio of lake sediments has been widely adopted as an indicator of weathering intensity in studies of past climate change, but the geochemical significance of this ratio varies with timescale. Here, we present Rb/Sr data for the past 300 years for sediments collected from Chaonaqiu Lake in the Liupan Mountains of the western Chinese Loess Plateau as a decadal-scale record of weathering intensity. To validate the application of this weathering proxy, we correlated the record with those of other major elements, rock-forming minerals, and paleoclimatic proxies. We found that Rb/Sr ratios are influenced mainly by Sr activity within the lake catchment (where Sr is likely sourced from albite). In addition, higher (lower) Rb/Sr ratios of bulk sediments from Chaonaqiu Lake are correlated with lower (higher) fractions of terrigenous detritus (SiO_2, Ti, K_2O, Al_2O_3, and Na_2O). These indicate that the Rb/Sr ratios of bulk sediments in Chaonaqiu Lake are closely linked to terrigenous detritus input on decadal scales and also correlate well with TOC (a precipitation indicator) and other high-resolution paleoclimate records (e.g., tree rings and drought/flood index) in neighboring regions, with higher (lower) Rb/Sr ratios corresponding to more (less) precipitation. Lake bulk sediment Rb/Sr ratios are dominated by the input of terrigenous detritus over decadal timescales. Our data show that physical and chemical weathering in the Chaonaqiu Lake watershed have opposing influences on Rb/Sr ratios of bulk sediment, competing to dominate these ratios of lake sediments over different timescales, with ratios reflecting the relative importance of the two types of weathering.

Keywords: Rb/Sr ratios; weathering intensity; decadal scales; Chaonaqiu Lake

check for updates

Citation: Liu, L.; Yu, K.; Li, A.; Zhang, C.; Wang, L.; Liu, X.; Lan, J. Weathering Intensity Response to Climate Change on Decadal Scales: A Record of Rb/Sr Ratios from Chaonaqiu Lake Sediments, Western Chinese Loess Plateau. *Water* **2023**, *15*, 1890. https://doi.org/10.3390/w15101890

Academic Editor: Achim A. Beylich

Received: 12 March 2023
Revised: 23 April 2023
Accepted: 5 May 2023
Published: 16 May 2023

1. Introduction

Numerous proxies based on ratios of elements have been used as indicators of past environmental and climatic change over various timescales [1–7]. The ratio of immobile to mobile elements usually indicates the intensity or degree of weathering [4,8,9]. Rubidium (Rb) tends to coexist with K in silicate minerals, such as K-feldspar, muscovite, biotite, etc., because the ionic radius of Rb is close to that of K. It exhibits inert behavior during weathering and is isolated in residual phases. Strontium (Sr) prefers Ca-bearing minerals, such as carbonate minerals, plagioclase, and pyroxene. When these minerals are subjected to weathering, the K-bearing minerals are generally more stable than Ca-bearing minerals, resulting in fractionation between Rb and Sr in weathering products [9]. The different behaviors of Rb and Sr in natural processes are helpful in identifying material sources and indicating chemical weathering intensity. Therefore, Rb/Sr ratios have been utilized for reconstructing the degree or intensity of chemical weathering and changes in climatic conditions over geological timescales [8–12]. For example, Rb/Sr ratios in Chinese loess/paleosoil profiles indicate the degree of weathering, where a higher Rb/Sr ratio corresponds to a higher degree of weathering and thus to stronger Asian summer monsoon intensity over long timescales, and vice versa [7,13–16]. On the other hand, the different geochemical behaviors of Rb and Sr in the process of terrestrial supergene weathering also provide a new idea for studying the records of trace elements in lake sediments. As a collector of watershed materials, lake sediments receive a large number of weathering products of rocks and soil in the basin. As the chemical weathering degree of rocks and soil in the basin increases, more Sr is leached from rocks and soil into the lake, and Rb remains in the original rocks and soil, resulting in a decrease in the Rb/Sr ratio of lake sediments. As a result, Rb/Sr ratios of lake sediments have been widely applied in the research field of lake paleoclimatology, often as an indicator of weathering intensity in catchments, where a lower Rb/Sr ratio of lake sediments indicates stronger chemical weathering in the basin, and vice versa [2–4,8,11,17,18]. For instance, Liu et al. [11] applied Rb/Sr ratios in reconstructing chemical weathering variability over the past 1200 years in the Gonghai Lake catchment, north China. Rb/Sr ratios in lacustrine sediments have also been adopted as an indicator of the evolution of Central Asia's westerly winds [19] and the Asian summer monsoon [11,20,21].

However, the factors affecting the material load transported into lakes can be complex and include the local climate, the chemical and physical properties of bedrock, and vegetation cover. Such factors may add complexity to the environmental interpretation of Rb/Sr ratios of lake sediments. For example, with strong physical loads in a catchment, although accompanying chemical weathering may be enhanced, the chemical composition of lake sediment may be mainly influenced by terrigenous detritus rather than chemical/biogenic deposition. Rb/Sr ratios of lake bulk sediment would in such a case serve primarily as an indicator of physical rather than chemical weathering intensity [9,22–24]. Rb/Sr ratios have also been regarded as an indicator of glacial conditions and lake water depth. For example, lower Rb/Sr ratios of sediments of the glacial Kalakuli Lake have been interpreted to indicate glacier advance, and vice versa [25]. Moreover, Rb/Sr ratios have been used as a proxy for water depth in lacustrine deposits in the Qaidam Basin [26]. It follows that an understanding of the controls on Rb/Sr ratios and their limitations is fundamental to their application and interpretation.

Chaonaqiu Lake is located in the Liupan Mountains on the western Chinese Loess Plateau in a zone that is transitional between semi-arid and semi-humid climatic conditions on the margin of the area affected by the modern Asian summer monsoon. An understanding of material transport from the catchment to the lake is critical in evaluating and predicting ecological and environmental changes, clarifying the environmental interpretation and significance of limnological indices, and elucidating weathering processes. Studies of Rb/Sr ratios of lake sediments may help to address these issues. Sediment cores recovered from Chaonaqiu Lake have yielded continuous varve sequences at high resolution with well-constrained chronology, and past changes in climate and vegetation have been reconstructed in detail on the basis of proxies such as total organic carbon (TOC) content [27], nitrogen stable isotope ratios ($\delta^{15}N$; [28]), n-alkanes [29], carbonate [30], and pollen records [31,32]. Recently, Zhang et al. [33] suggested that Rb/Sr ratios in Chaonaqiu Lake sediments may be controlled by chemical weathering intensity on centennial–millennial scales, although the exact weathering processes were not discussed. This study focuses on the environmental geochemical significance of Rb/Sr ratios in Chaonaqiu Lake sediments on decadal timescales based on the characteristics, geographical location, and significance of multiple proxies and considers the relevant weathering process on different timescales.

2. Materials and Methods

2.1. Study Area

Chaonaqiu Lake (latitude 35°16′ N, longitude 106°19′ E, altitude 2430 m a.s.l.) is located in the Liupan Mountains, ~30 km to the northeast of Zhuanglang County (Figure 1a). It has a surface area of 0.02 km^2 with a maximum water depth of 10 m. Chaonaqiu Lake is an alpine-barrier freshwater lake with a seasonal outflow on its western margin (Figure 1b), and the lake water is supplied mainly by precipitation. The bedrock of the catchment basin of the lake is red sandstone. The pH and salinity of the lake water are 7.83 and 0.17 g L^{-1}, respectively [34], while total P and N concentrations are 40.2 and 1096.8 μg L^{-1}, respectively [28]. Meteorological records for 1960–2007 from the nearby Zhuanglang meteorological station indicate a mean annual temperature (MAT) of 8.1 °C, with mean temperatures for January and July of −5.2 °C and 20.1 °C, respectively (Figure 1c). The mean annual precipitation is 513 mm, with ~70% falling in summer (June–September; Figure 1c).

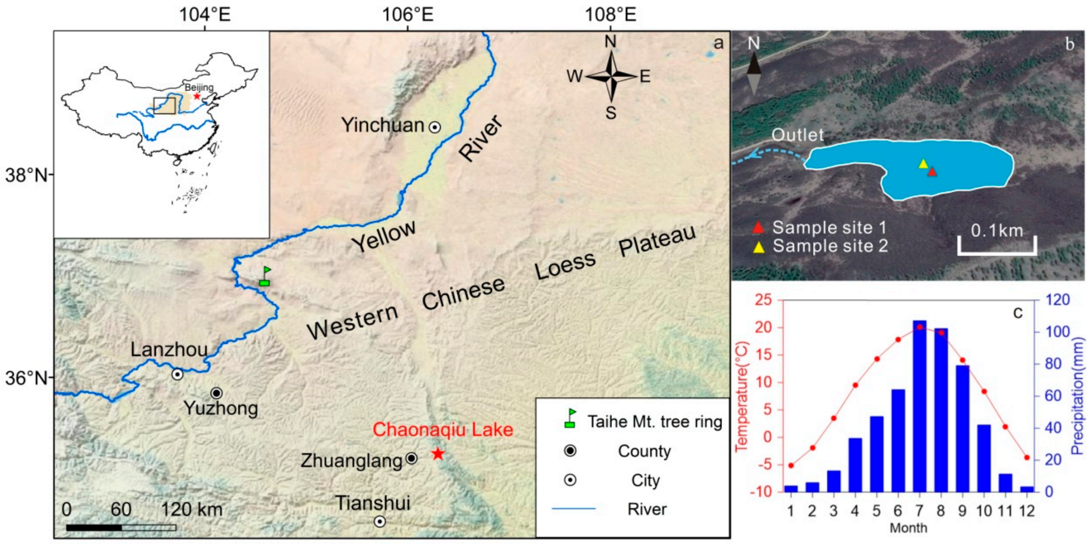

Figure 1. Location and setting. (**a**) Location of our study site, Chaonaqiu Lake, in the south-western Chinese Loess Plateau, and other previous studies mentioned in the text include the Taihe Mt. tree ring and the Yuzhong and Tianshui drought/flood (D/F) index. (**b**) Satellite image of the Chaonaqiu Lake (maps modified from Google Earth) and the location of sampling site. (**c**) Mean monthly temperature (red dotted line) and precipitation (blue bars) from Zhuanglang meteorological station based on 1960–2007 data from China Meteorological Administration.

2.2. Sampling

In September 2012, four surface sediment cores, designated CNQ12–1, CNQ12–2, CNQ12–3, and CNQ12–4, were retrieved from the center of Chaonaqiu Lake using a gravity corer (UWITEC, Austria). Cores CNQ12–1 (~73 cm) and CNQ12–2 (~130 cm) were retrieved from Site 1, and cores CNQ12–3 (~70 cm) and CNQ12–4 (~138 cm) were retrieved from Site 2 (Figure 1b). Sediment profiles were undisturbed, with a clear interface between sediment and water. Core CNQ12–1 was subsampled in the field at an interval of 1 cm to quantify the core mass depth for constructing an accurate chronological model. Core CNQ12–4 was subsampled in the laboratory at an interval of 1 cm. The core CNQ12–1 was used for this study.

2.3. Chronology Control

^{137}Cs and $^{210}Pb_{ex}$ radioactivity of core CNQ12–1 was determined through HpGe (GWL-250-15 detector; Ortec, Atlanta, GA, USA) high-resolution gamma spectrometry, with an experimental error of <10% and a detection limit of 0.1 Bq kg^{-1} at a 99% confidence level [35], at the Institute of Earth Environment, Chinese Academy of Sciences, Xi'an, China. The dating results have been reported by Ref. [27].

2.4. Experiment and Statistical Analysis

Thirty-seven subsamples from core CNQ12–1 were selected for traditional XRF analysis by X-ray fluorescence spectrometry (XRF; PW440, Axios advanced, The Netherlands; [36]). For this, ~1 g of dried sample powder was calcined in a muffle furnace at 550 °C to remove organic matter, and 0.6 g of subsamples was mixed with 6 g dry lithium tetraborate ($Li_2B_4O_7$) for fusion to glass in a platinum crucible at 1000 °C. Calibrations involved 4 Chinese soil samples (GSS1~4) with analytical uncertainties of ±3% for major elements. Twenty-six representative sediment samples from core CNQ12–1 and one surface soil sample from the catchment were selected for X-ray diffraction (XRD) analysis (details see [30]) to obtain mineral assemblages and elemental geochemical characteristics of sediments. All analyses were undertaken at the Institute of Earth Environment, Chinese Academy of Sciences, Xi'an, China.

We used SPSS 17.0 software to conduct Pearson correlation analysis on experimental data and other related data. Considering the differences in the number of samples for each experimental indicator, all data were symmetrized based on the sample number before correlation analysis to ensure the accuracy and scientificity of the results.

3. Results

3.1. Chronology

Based on the age model, the core CNQ12–1 has a constant mass accumulation rate (MAR) of 0.0852 $g \cdot cm^{-2} \cdot yr^{-1}$ over the period of 1743–2012 (refer to [27] for details). The ^{137}Cs–^{210}Pb ages of Chen et al. [28] and Guo et al. [32] from Chaonaqiu Lake are also plotted in Figure 2 and correlate well with those of our dating model (Figure 2). In addition, the ^{14}C age of 500 cal yr BP occurs at 100 cm depth [32] and 620 cal yr BP at 162 cm depth in Chaonaqiu Lake [29,37], consistent with our ^{137}Cs age model. The close correspondence of these various age constraints confirms that our presented chronology is reliable.

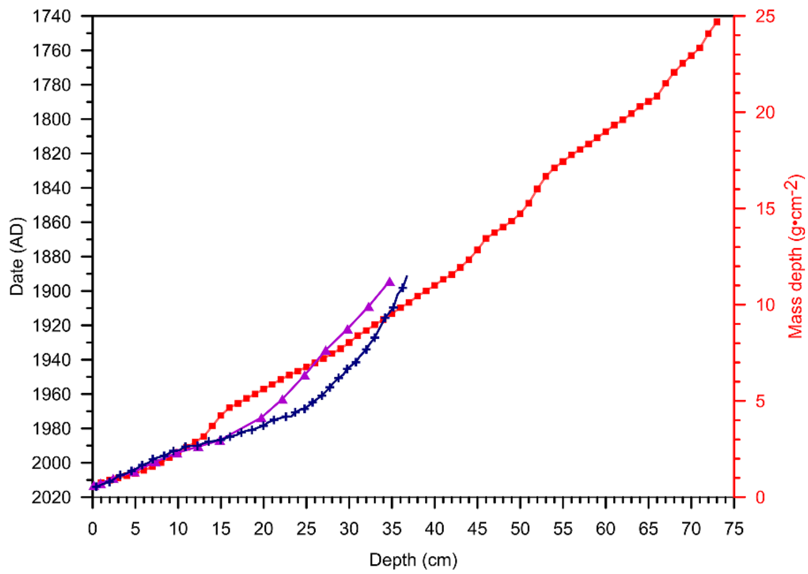

Figure 2. Chronologies for core CNQ12–1 (red curve, our ^{137}Cs age model; refer to [27] for details), core GS14A (purple curve, $^{137}Cs-^{210}Pb$ age model; [28]) and that reported by Guo et al. [32] (blue curve, $^{137}Cs-^{210}Pb$ age model).

3.2. Elemental Geochemical and Mineral Assemblages

The Rb contents of core CNQ12–1 are in the range of 176.1–246.5 ppm with an average of 200.8 ppm, while Sr contents are in the range of 175.6–236.6 ppm with an average of 203.58 ppm. Rb/Sr ratios range from 0.78 to 1.29 with an average of 0.99 (Figure 3). Rb and Sr display generally opposing trends at 1–15 cm and 55–73 cm depths in the profile but are consistent at 15–55 cm. Rb/Sr ratios are negatively correlated with Sr (Pearson correlation coefficient $r = -0.703$, $p = 0.01$; Table 1) and positively correlated with Rb (Pearson correlation coefficient $r = 0.623$, $p = 0.01$; Table 1) contents (Figure 3). This suggests that the variation in Rb/Sr ratios depends primarily on Sr element activity during weathering.

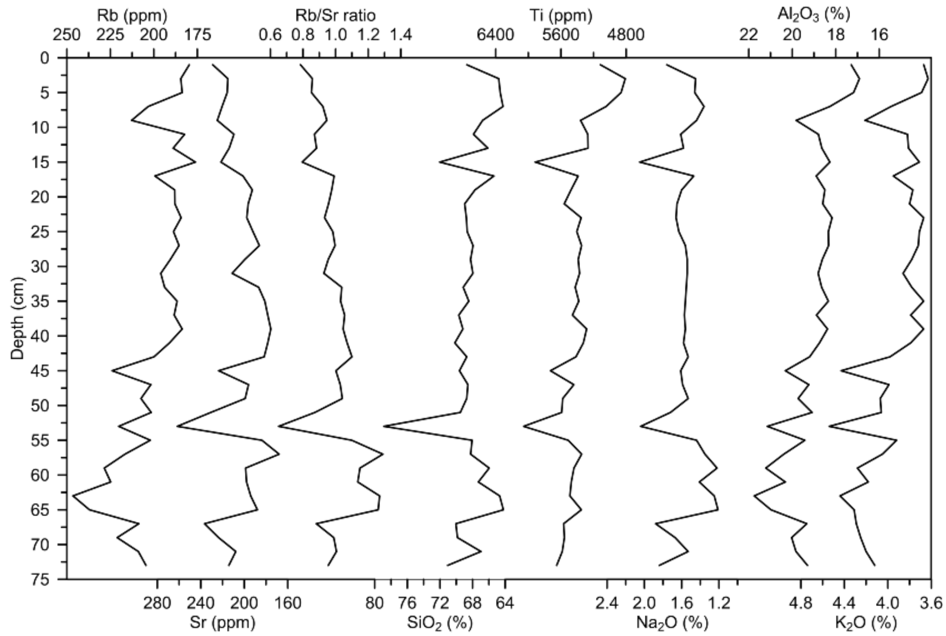

Figure 3. XRF analysis results for core CNQ12–1. SiO_2 data are from [27].

Table 1. Pearson correlation coefficients between species in sediments from core CNQ12–1.

Pearson Correlation / Sig. (2-Tailed)	Ti	Na_2O	Al_2O_3	K_2O	Rb	Sr	Rb/Sr
SiO_2	0.686 **	0.817 **	0.134	0.163	*−0.095*	0.340 *	*−0.303*
	0.000	0.000	0.430	0.334	0.574	0.039	0.068
Ti		0.409 *	0.659 **	0.630 **	0.449 **	0.210	0.153
		0.012	0.000	0.000	0.005	0.213	0.365
Na_2O			*−0.258*	*−0.094*	*−0.407 **	0.543 **	*−0.698 ***
			0.123	0.581	0.012	0.001	0.000
Al_2O_3				0.896 **	0.919 **	0.034	0.633 **
				0.000	0.000	0.843	0.000
K_2O					0.920 **	0.385 *	0.353 *
					0.000	0.019	0.032
Rb						0.111	0.623 **
						0.511	0.000
Sr							*−0.703 ***
							0.000

Note: N = 37. * Significant at $p = 0.05$. ** Significant at $p = 0.01$. Bold and italic fonts indicate positive and negative correlations, respectively. SiO_2 data are from [27].

Overall, element and oxide contents are strongly correlated in core CNQ12–1 (Figure 3; Table 1). Rb contents are positively correlated with those of Ti, K_2O, and Al_2O_3, especially with K_2O and Al_2O_3 ($r > 0.90$; Table 1); Sr contents are significantly and positively correlated with SiO_2, K_2O, and Na_2O contents; and Rb/Sr ratios are similarly correlated with

Al_2O_3, K_2O, and Na_2O contents (Table 1). Si, Al, K, and Ti contents of lake sediments are generally considered to be associated with the influx of exogenous clastic materials [38,39] and are positively correlated with each other in Chaonaqiu Lake sediments (Figure 3; Table 1), reflecting their similar characteristics, sources, and transport and sedimentation processes [40].

Our XRD analyses reveal that core CNQ12–1 has a mineralogic composition that is dominated by quartz, biotite, albite, chlorite, and calcite (Figure 4). Except for calcite, the close correspondence of mineralogic compositions and primary peaks between surface soils and lake sediments implies that sediments in Lake Chaonaqiu are sourced primarily from terrestrial clastic material. The element compositions of these minerals in sediment are similar to the elements listed in Table 1, indicating that these elements have similar characteristics, sources, and transportation and sedimentation processes [40].

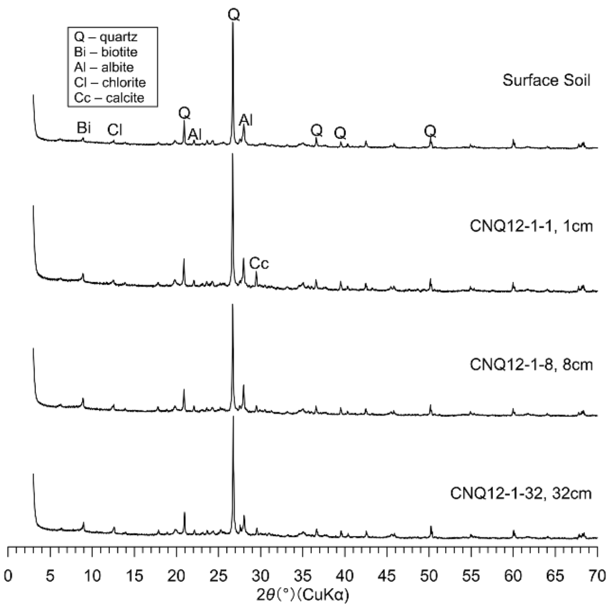

Figure 4. Results of XRD analysis for core CNQ12–1 and surface soils.

4. Discussion

4.1. Environmental Geochemical Significance of the Rb/Sr Ratio in the Chaonaqiu Lake

Under natural conditions, Sr-bearing minerals in lake sediments are derived from two sources: terrigenous detritus (directly brought in by physical erosion) and dissolved materials (produced by chemical weathering). If the Rb/Sr ratios in bulk sediments are controlled mainly by physical loads, then more intense physical weathering should be correlated with higher contents of terrigenous detritus, with lower Rb/Sr ratios [22,23]. In contrast, if the Rb/Sr ratios in bulk sediments are mainly determined by chemical weathering, more intense chemical weathering is expected to be correlated with higher Sr contents and lower Rb/Sr ratios [3,4,8,11,17,18]. Therefore, Rb/Sr ratios of lake sediments reflect the competition between (i.e., the relative importance of) physical weathering and chemical weathering [9]. Where Sr in sediments occurs mainly in coarse terrigenous clastic minerals (e.g., feldspar minerals), the Rb/Sr ratio reflects the intensity of physical transport within the basin [3,22]. XRD analyses show that the minerals in lake sediments and surface soil are dominated by quartz, albite, biotite, and chlorite (Figure 4), with the calcite in sediments being authigenic [30]. As shown in Figure 5, the trend of Sr content is consistent with that of albite signal strength (Figure 5), and there is a significant positive correlation between them (Pearson correlation coefficients $r = 0.777$, $p = 0.01$; Table 2). In contrast, the trends in Sr content are not consistent with that of calcite signal strength, and although there is a positive correlation between them, the Pearson correlation coefficient ($r = 0.134$; Table 2) is much lower than that for albite. These results imply that Sr is likely enriched in albite. Rb/Sr ratios are also strongly correlated with the content of the terrigenous fraction (SiO_2, Ti, K_2O, Al_2O_3, and Na_2O; Table 1 and Figure 3), implying that the Rb/Sr ratios in sediments of Chaonaqiu Lake are likely dominated by terrigenous detritus and, therefore, that physical weathering predominated within the catchment of the lake. This is similar to the results observed in Lake Qinghai [9] and Lake Teletskoye [22,23].

Table 2. Pearson correlation coefficients among Sr and other proxies or indicators from core CNQ12–1.

Pearson Correlation / Sig. (2-Tailed) / N	albite	calcite	TOC	TCC
Sr	**0.777** ** 0.000 26	0.134 0.514 26	**−0.570** ** 0.000 37	0.004 0.981 37
albite		/ / /	**0.618** ** 0.001 26	0.007 0.972 26
calcite			/ / /	**0.803** ** 0.000 26
TOC				0.248 0.139 37

Note: ** Significant at $p = 0.01$. Bold fonts indicate significant correlation. TOC (total organic carbon, a precipitation indicator) data from [27], TCC (total carbonate content, a temperature indicator) and calcite data are all from [30].

Chaonaqiu Lake is situated in the Liupan Mountains, in the western Chinese Loess Plateau, which is in the transitional zone between a semi-arid and semi-humid climate, with significant annual and daily temperature differences [41]. Although the mean annual precipitation (513 mm) in the Chaonaqiu Lake basin reflects a semi-humid climatic environment, the precipitation distribution is uneven (~70% occurs during summer, often in heavy rainstorms) because the climate zonation of the Loess Plateau has not changed [42,43]. Therefore, regardless of whether total annual precipitation increases or decreases, local precipitation characteristics do not change. During wetter intervals, more precipitation increases the vegetation cover in the watershed, which stabilizes soil and also reduces the sediment-carrying capacity of runoff, resulting in less terrigenous detritus entering into the lake and higher Rb/Sr ratios in bulk sediments. During drier periods, less precipitation decreases the vegetation cover in the watershed, and the sparse vegetation cover results in more surface soil in the watershed being exposed, producing a less cohesive soil such that even low-intensity rainfall may generate a higher sediment-carrying capacity of runoff with increased terrigenous detritus transport and lower Rb/Sr ratios of lake sediments.

4.2. Comparison of the Rb/Sr Ratio with Other Precipitation Indicators and Records

The organic matter in lake sediments mainly includes endogenous organic matter (produced by aquatic plants and planktonic algae in the lake) and terrestrial organic matter (from plants growing in the watershed) [40,44,45]. According to our previous work, TOC contents in Chaonaqiu Lake have been demonstrated to indicate local precipitation variations [27]. In wetter climatic conditions, more precipitation increases the vegetation coverage in the watershed, leading to relatively more terrestrial organic matter being transported into the lake and therefore to higher TOC content [27]. On the other hand, in drier climatic conditions, less precipitation decreases the vegetation coverage in the watershed, resulting in relatively less terrestrial-derived organic matter being transported into the lake and therefore lower TOC content [27]. We found that the trend of Sr content is opposite to that of TOC (Figure 5) and found a significant negative correlation between Sr contents and TOC contents (Pearson correlation coefficient $r = -0.570$, $p = 0.01$; Table 2), while the correlation between Sr contents and TCC (total carbonate contents, as a temperature indicator [30]) is much lower than that with TOC contents (Pearson correlation coefficient *r* = 0.004; Table 2), even though there is a positive correlation between them. This reveals that the Sr contents in the sediments of Chaonaqiu Lake were mainly controlled by precipitation rather than temperature on decadal scales such that more precipitation is correlated with lower Sr contents and thus higher Rb/Sr ratios and less precipitation correlated to higher Sr contents and therefore lower Rb/Sr ratios.

As shown in Figure 5, the temporal trends in Rb/Sr ratios and other indices (e.g., SiO_2 content and albite signal strength) in core CNQ12–1 are generally similar to those of the precipitation indicator (e.g., TOC; [27]) and records from Taihe Mt. tree rings [46] and the drought/flood (D/F) index [47–49] in neighboring regions on decadal scales. The Rb/Sr ratios exhibited five lower value phases (e.g., 1770–1780 AD, 1830–1845 AD, 1870–1880 AD, 1925–1935 AD, and 1970–1980 AD; see cyan shadings in Figure 5) over the past 300 years, implying strong physical weathering in these five intervals. For example, the Rb/Sr ratios showed the lowest value (highest Sr contents) during the period of 1830–1845 AD, suggesting strong physical weathering (Figure 5). The TOC contents exhibited a lower value during the same period, which implied a drier climate condition, and both Taihe Mt. tree rings [46] and the Drought/Flood (D/F) index [47–49] in neighboring regions also identified drier conditions during this interval. The arid environment resulted in an enhancement in physical weathering, which caused more albite and Sr to be transported into the lake, leading to a lower Rb/Sr ratio during this episode (Figure 5).

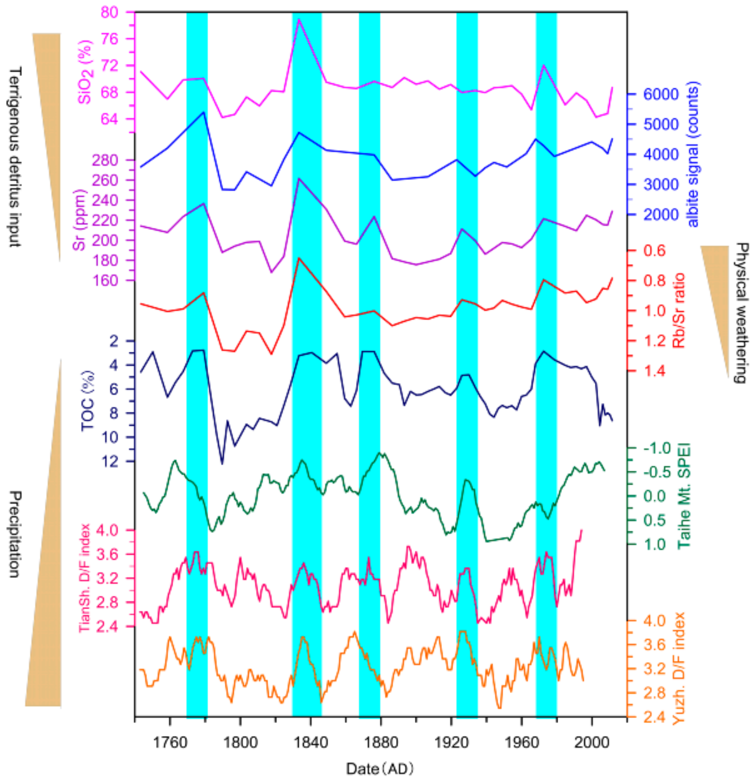

Figure 5. Comparison of the Rb/Sr ratio with other indices of core CNQ12–1 in Chaonaqiu Lake and other precipitation records in neighboring regions. The TOC (total organic carbon) is a precipitation indicator (higher value indicates a wetter climate condition, and vice versa; see [27] for details). The smoothed curve of Taihe Mt. SPEI (standardized precipitation evapotranspiration index, where higher value indicates a wetter climate condition; [46]) and the D/F index (higher value indicates a drier climate condition, and vice versa; [47–49]) are all 11-year running means. The cyan shadings indicate dry intervals.

4.3. Response of Weathering Intensity to Climate Change on Different Timescales

As physical weathering decreases in the Chaonaqiu Lake catchment over short (decadal) timescales, the chemical weathering intensity likely increases with precipitation, but water–rock reactions may weaken with less terrigenous material being involved. This implies that during wet intervals, although the intensity of chemical weathering increases, the amounts of Sr-bearing minerals chemically/biogenically deposited in sediments would decrease, not increase. Increased chemical weathering would thus be correlated with higher Rb/Sr ratios over short timescales. The Rb/Sr ratios of lake sediments are affected mainly by terrigenous detritus input, reflecting environmental conditions on short timescales [3]. This effect is recorded with high resolution because the terrigenous detritus sinks rapidly to the lake bottom.

In comparison, over long timescales (millennium scales), chemical weathering is likely to be more important than physical weathering in regulating long-term trends in sediment Rb/Sr ratios. Zeng et al. [3] and Xu et al. [9] considered that if the Rb/Sr ratios in lake sediment are used as an indicator of chemical weathering, it may reflect environmental trends on long timescales (i.e., low resolution) because chemical weathering is a continuous and gradual process affected by both climatic factors and the lake water hydrochemical environment. Our previous study found that the carbonate in the sediments of Chaonaqiu Lake is authigenic and derived mainly from calcite [30]. The rate of autogenic carbonate deposition in Chaonaqiu Lake is influenced by temperature-controlled water salinity, and long-timescale records of Sr contents (and hence Rb/Sr ratios) should be the result of the co-dominance of precipitation and temperature. Therefore, there is a relationship between precipitation and Rb/Sr ratio as follows: a "more precipitation~lower Rb/Sr ratio" relationship applies over long terms (e.g., centennial–millennial scales; [33]), while a "more precipitation~higher Rb/Sr ratio" relationship applies over short terms (e.g., decadal scales, as shown in Figure 5). Hence, the interpretation of the environmental geochemical significance of Rb/Sr ratios of lake sediments must consider the timescale involved.

5. Conclusions

Rb and Sr in lacustrine sediments originate from terrigenous detritus and dissolved materials. The environmental geochemical significance of Rb/Sr ratios in bulk sediments of Chaonaqiu Lake was investigated in this paper. We have drawn conclusions as follows:

(1) The trend of Sr concentration is consistent with that of albite signal strength rather than that of calcite, and there is a significant positive correlation between them. This implies that Sr is likely sourced from albite rather than calcite. The correlation between Rb/Sr ratios and Sr concentration is higher than that with Rb concentration, indicating that the variation in Rb/Sr ratios depends mainly on Sr activity within the lake catchment. The Rb/Sr ratio in the sediment of Chaonaqiu Lake may be closely linked to terrigenous detritus input from the watershed on decadal scales, which is determined by physical weathering in the watershed of the lake.

(2) The Rb/Sr ratios identified five lower value intervals (e.g., 1770–1780 AD, 1830–1845 AD, 1870–1880 AD, 1925–1935 AD, and 1970–1980 AD), implying stronger physical weathering during these periods. These correlate well with lower TOC contents in the sediments, a lower tree-ring SPEI, and a higher D/F index in neighboring regions, suggesting strong physical weathering due to drier climate conditions on decadal scales.

(3) Physical weathering and chemical weathering in the Chaonaqiu Lake catchment have opposing influences on the sediment Rb/Sr ratio and may compete on different timescales for dominant control. Investigation of temporal trends in Rb/Sr ratios is necessary, especially on short timescales, before their application in studies of catchment weathering intensity.

Author Contributions: Methodology, L.L., K.Y., A.L., C.Z., L.W. and X.L.; Writing—original draft preparation, L.L.; Writing—review and editing, K.Y. and J.L. All authors have read and agreed to the published version of the manuscript.

Funding: This work was funded by the Natural Science Foundation of China (42277455, 42273060, and 41701032), the Project of State Key Laboratory of Loess and Quaternary Geology (SKLLQG2119, SKLLQGPY2104), the Ph.D. Research Project of Baoji University of Arts and Sciences (ZK2017046), and the Youth Innovation Promotion Association of the Chinese Academy of Sciences (2021411).

Data Availability Statement: Data of this research are available in the East Asian Paleoenvironmental Science Database (http://paleodata.ieecas.cn/index_EN.aspx) (accessed on 11 March 2023).

Conflicts of Interest: The authors declare no conflict of interest.

References

1. Morellón, M.; Valero-Garcés, B.; Vegas-Vilarrúbia, T.; González-Sampériz, P.; Romero, Ó.; Delgado-Huertas, A.; Mata, P.; Moreno, A.; Rico, M.; Corella, J.P. Lateglacial and Holocene palaeohydrology in the western Mediterranean region: The Lake Estanya record (NE Spain). *Quat. Sci. Rev.* **2009**, *28*, 2582–2599. [CrossRef]
2. Zeng, Y.; Chen, J.A.; Zhang, W.; Zhu, Z.J.; Li, J. The non-residual Rb/Sr ratio of the Huguangyan Maar Lake and its implications for paleoclimate change. *Geochimica* **2011**, *40*, 249–257. (In Chinese with English abstract)
3. Zeng, Y.; Chen, J.A.; Zhu, Z.J.; Li, J. Advance and Porspective of Rb/Sr Ratios in Lake Sediments as an Index of Paleoclimate/Paleoenvironment. *Adv. Earth Sci.* **2011**, *26*, 805–810. (In Chinese with English abstract)
4. Zeng, Y.; Chen, J.A.; Xiao, J.L.; Qi, L. Non-residual Sr of the sediments in Daihai Lake as a good indicator of chemical weathering. *Quat. Res.* **2013**, *79*, 284–291. [CrossRef]
5. Croudace, I.W.; Rothwell, R.G. *Micro-XRF Studies of Sediment Cores. Developments in Paleoenvironmental Research*; Springer: Berlin, Germany, 2015; pp. 189–226.
6. Tian, J.C.; Zhang, X. *Sedimentary Geochemistry*; Geology Press: Beijing, China, 2016; pp. 67–68. (In Chinese)
7. Liu, X.X.; Sun, Y.B.; Vandenberghe, J.; Cheng, P.; Zhang, X.; Gowan, E.J.; Lohmann, J.; An, Z.S. Centennial- to millennial-scale monsoon changes since the last deglaciation linked to solar activities and North Atlantic cooling. *Clim. Past.* **2020**, *16*, 315–324. [CrossRef]
8. Jin, Z.D.; Cao, J.; Wu, J.; Wang, S. A Rb/Sr record of catchment weathering response to Holocene climate change in Inner Mongolia. *Earth Surf. Proc. Landf.* **2006**, *31*, 285–291. [CrossRef]
9. Xu, H.; Liu, B.; Wu, F. Spatial and temporal variations of Rb/Sr ratios of the bulk surface sediments in Lake Qinghai. *Geochem. Trans.* **2010**, *11*, 3. Available online: https://doi.org/10.1186/1467-4866-11-3 (accessed on 9 July 2010). [CrossRef] [PubMed]
10. Wu, Y.H.; Lücke, A.; Jin, Z.D.; Wang, S.M.; Schleser, G.H.; Battarbee, R.W.; Xia, W.L. Holocene climate development on the central Tibetan Plateau: A sedimentary record from Cuoe Lake. *Palaeogeogr. Palaeoclimatol. Palaeoecol.* **2006**, *234*, 328–340. [CrossRef]
11. Liu, J.B.; Chen, J.H.; Selvaraj, K.; Xu, Q.; Wang, Z.; Chen, F. Chemical weathering over the last 1200 years recorded in the sediments of Gonghai Lake, Lvliang Mountains, North China: A high-resolution proxy of past climate. *Boreas* **2014**, *43*, 914–923. [CrossRef]
12. Fritz, M.; Unkel, I.; Lenz, J.; Gajewski, K.; Frenzel, P.; Paquette, N.; Lantuit, H.; Körte, L.; Wetterich, S. Regional environmental change versus local signal preservation in Holocene thermokarst lake sediments: A case study from Herschel Island, Yukon (Canada). *J. Paleolimnol.* **2018**, *60*, 77–96. [CrossRef]
13. Chen, J.; An, Z.S.; Head, J. Variation of Rb/Sr Ratios in the Loess-Paleosol Sequences of Central China during the Last 130,000 Years and Their Implications for Monsoon Paleoclimatology. *Quat. Res.* **1999**, *51*, 215–219. [CrossRef]
14. Chen, J.; An, Z.S.; Liu, L.W.; Ji, J.F.; Yang, J.D.; Chen, Y. Variations in chemical compositions of the eolian dust in Chinese Loess Plateau over the past 2.5 Ma and chemical weathering in the Asian inland. *Sci. China Ser. D Earth Sci.* **2001**, *31*, 136–145. (In Chinese) [CrossRef]
15. Sun, J.M. Provenance of loess material and formation of loess deposits on the Chinese Loess Plateau. *Earth Planet. Sci. Lett.* **2002**, *203*, 845–859. [CrossRef]
16. Guo, F.; Wang, T.; Liu, Y.M.; Wang, Y.; Fan, H.M.; Sun, Y.B. Rapid Asian monsoon changes record by Loess depositions in Linxia since 260 ka B.P. *Quat. Sci.* **2019**, *39*, 558–564. (In Chinese with English abstract)
17. Jin, Z.D.; Wang, S.M.; Shen, J.; Zhang, E.L.; Li, F.C.; Ji, J.F.; Lu, X.W. Chemical weathering since the Little Ice Age recorded in lake sediments: A high-resolution proxy of past climate. *Earth Surf. Proc. Landf.* **2001**, *26*, 775–782. [CrossRef]
18. Yang, H.F.; Zhao, Y.; Cui, Q.Y.; Ren, W.H.; Li, Q. Paleoclimatic indication of X-ray fluorescence core-scanned Rb/Sr ratios: A case study in the Zoige Basin in the eastern Tibetan Plateau. *Sci. China Earth Sci.* **2021**, *64*, 80–95. [CrossRef]
19. Chang, H.; An, Z.S.; Wu, F.; Jin, Z.D.; Liu, W.G.; Song, Y.G. A Rb/Sr record of the weathering response to environmental changes in westerly winds across the Tarim Basin in the late Miocene to the early Pleistocene. *Palaeogeogr. Palaeoclimatol. Palaeoecol.* **2013**, *386*, 364–373. [CrossRef]
20. An, Z.S.; Steven, C.C.; Shen, J.; Qiang, X.K.; Jin, Z.D.; Sun, Y.B.; Warren, L.P.; Luo, J.J.; Wang, S.M.; Xu, H.; et al. Glacial-interglacial Indian summer monsoon dynamics. *Science* **2011**, *333*, 719–723. [CrossRef]
21. Zhao, Y.; Tzedakis, P.C.; Li, Q.; Qin, F.; Cui, Q.Y.; Liang, C.; Birks, H.; Liu, Y.L.; Zhang, Z.Y.; Ge, J.Y.; et al. Evolution of vegetation and climate variability on the Tibetan Plateau over the past 1.74 million years. *Sci. Adv.* **2020**, *6*, eaay6193. [CrossRef]
22. Kalugin, I.; Daryin, A.; Smolyaninova, L.; Andreev, A.; Diekmann, B.; Khlystov, O. 800-yr-long records of annual air temperature and precipitation over southern Siberia inferred from Teletskoye Lake sediments. *Quat. Res.* **2007**, *67*, 400–410. [CrossRef]

23. Kalugin, I.; Selegei, V.; Goldberg, E.; Seret, G. Rhythmic fine-grained sediment deposition in Lake Teletskoye, Altai, Siberia, in relation to regional climate change. *Quat. Int.* **2005**, *136*, 5–13. [CrossRef]
24. Ren, X.P.; Nie, J.S.; Saylor, J.E.; Li, H.; Bush, M.A.; Horton, B.K. Provenance control on chemical weathering index of fluvio-lacustrine sediments: Evidence from the Qaidam Basin, NE Tibetan Plateau. *Geochem. Geophys. Geosyst.* **2019**, *20*, 3216–3224. [CrossRef]
25. Liu, X.Q.; Herzschuh, U.; Wang, Y.B.; Kuhn, G.; Yu, Z.T. Glacier fluctuations of muztagh ata and temperature changes during the late Holocene in westernmost Tibetan Plateau, based on glaciolacustrine sediment records. *Geophys. Res. Lett.* **2014**, *41*, 6265–6273. [CrossRef]
26. Chang, F.Q.; Zhang, H.C.; Lei, G.L.; Pu, Y.; Chen, G.J.; Zhang, W.X.; Yang, L.Q. Geochemical behaviors of strontium isotope and related elements of the lacustrine deposits and their application to paleoenvironment reconstruction. *Quat. Sci.* **2010**, *30*, 962–971. (In Chinese with English abstract)
27. Yu, K.K.; Xu, H.; Lan, J.H.; Sheng, E.G.; Liu, B.; Wu, H.X.; Tan, L.C.; Yeager, K.M. Climate change and soil erosion in a small alpine lake basin on the Loess Plateau, China. *Earth Surf. Proc. Landf.* **2017**, *42*, 1238–1247. [CrossRef]
28. Chen, J.; Liu, J.; Xie, C.; Chen, G.; Chen, J.; Zhang, Z.; Zhou, A.; Rühland, K.; Smol, J.P.; Chen, F. Biogeochemical responses to climate change and anthropogenic nitrogen deposition from a 200-year record from Tianchi Lake, Chinese Loess Plateau. *Quat. Int.* **2018**, *493*, 22–30. [CrossRef]
29. Sun, H.L.; James, B.; Osamu, S.; Zhou, A.F. Mid- to- late Holocene hydroclimatic changes on the Chinese Loess Plateau: Evidence from n-alkanes from the sediments of Tianchi Lake. *J. Paleolimnol.* **2018**, *60*, 511–523. [CrossRef]
30. Yu, K.K.; Wang, L.; Liu, L.P.; Sheng, E.G.; Liu, X.X.; Lan, J.H. Temperature variations and possible forcing mechanisms over the past 300 years recorded at Lake Chaonaqiuqiu in the Western Loess Plateau. *Sustainability* **2021**, *13*, 11376. [CrossRef]
31. Zhao, Y.; Chen, F.H.; Zhou, A.F.; Yu, Z.C.; Zhang, K. Vegetation history, climate change and human activities over the last 6200 years on the Liupan Mountains in the southwestern Loess Plateau in central China. *Palaeogeogr. Palaeoclimatol. Palaeoecol.* **2010**, *293*, 197–205. [CrossRef]
32. Guo, C.; Ma, Y.Z.; Meng, H.W. Late Holocene vegetation, climate, and lake changes in northern China: Varved evidence from western Loess Plateau. *Sci. Total Environ.* **2022**, *827*, 154282. [CrossRef]
33. Zhang, H.; Niu, L.L.; Yuan, Z.J.; Zhang, C.; Sun, H.L.; Zhang, X.J.; Zhou, A.F. Mid-late Holocene soil erosion record from lake deposit of Liupan Mountains. *J. Earth Environ.* **2021**, *12*, 146–158. (In Chinese with English abstract)
34. Xu, H.; Yu, K.K.; Lan, J.H.; Sheng, E.G.; Liu, B.; Ye, Y.D.; Hong, B.; Wu, H.X.; Zhou, K.E.; Yeager, K.M. Different responses of sedimentary $\delta^{15}N$ to climatic changes and anthropogenic impacts in lakes across the Eastern margin of the Tibetan Plateau. *J. Asian Earth Sci.* **2016**, *123*, 111–118. [CrossRef]
35. Lan, J.; Wang, T.; Chawchai, S.; Cheng, P.; Xu, H. Time marker of ^{137}Cs fallout maximum in lake sediments of Northwest China. *Quat. Sci. Rev.* **2020**, *241*, 106413. [CrossRef]
36. Xu, H.; Zhou, X.; Lan, J.; Liu, B.; Sheng, E.; Yu, K.; Cheng, P.; Wu, F.; Hong, B.; Yeager, K.M. Late Holocene Indian summer monsoon variations recorded at Lake Erhai, Southwestern China. *Quat. Res.* **2015**, *83*, 307–314. [CrossRef]
37. Zhang, C.; Zhou, A.F.; Zhang, H.X.; Zhang, Q.; Zhang, X.N.; Sun, H.L.; Zhao, C. Soil erosion in relation to climate change and vegetation cover over the past 2000 years as inferred from the Tianchi lake in the Chinese Loess Plateau. *J. Asian Earth Sci.* **2019**, *180*, 103850. [CrossRef]
38. Yancheva, G.; Nowaczyk, N.R.; Mingram, J.; Dulski, P.; Schettler, G.; Negendank, J.F.W.; Liu, J.; Sigman, D.M.; Peterson, L.C.; Haug, G.H. Influence of the intertropical convergence zone on the East Asian monsoon. *Nature* **2007**, *445*, 74–77. [CrossRef]
39. Kylander, M.E.; Ampel, L.; Wohlfarth, B.; Veres, D. High-resolution X-ray fluorescence core scanning analysis of Les Echets (France) sedimentary sequence: New insights from chemical proxies. *J. Quat. Sci.* **2011**, *26*, 109–117. [CrossRef]
40. Shen, J.; Xue, B.; Wu, J.L.; Wu, Y.H.; Liu, X.Q.; Yang, X.D.; Liu, J.; Wang, S.M. *Lake Sedimentation and Environmental Evolution*; Science Press: Beijing, China, 2010; pp. 74–81. (In Chinese)
41. Cheng, J.M.; Yu, Z.J.; Zhu, R.B.; Jin, J.W.; Jing, Z.B. *Comprehensive Scientific Investigation Report of Liupan Mountains National Nature Reserve*; Science Press: Beijing, China, 2013; pp. 7–8. (In Chinese)
42. Wang, X.Q.; Jin, Z.D.; He, Z.; Zhou, L.; Xu, J.W. New insights into dating the sediment sequence within a landslide-dammed reservoir on the Chinese Loess Plateau. *Holocene* **2019**, *29*, 1020–1029. [CrossRef]
43. Wang, X.Q.; Wang, Z.S.; Xiao, J.; He, M.Y.; Zhang, F.; Pan, Y.H.; Zhang, Y.X.; Jin, Z.D. Soil erosion fluxes on the central Chinese Loess Plateau during CE 1811 to 1996 and the roles of monsoon storms and human activities. *Catena* **2021**, *200*, 105148. [CrossRef]
44. Xu, H.; Ai, L.; Tan, L.C.; An, Z.S. Stable isotopes in bulk carbonates and organic matter in recent sediments of Lake Qinghai and their climatic implications. *Chem. Geol.* **2006**, *235*, 262–275. [CrossRef]
45. Meyers, P.A. Preservation of elemental and isotopic source identification of sedimentary organic matter. *Chem. Geol.* **1994**, *114*, 289–302. [CrossRef]
46. Ma, Y.Y.; Liu, Y.; Song, H.M.; Sun, J.Y.; Lei, Y.; Wang, Y.C. A standardized precipitation evapotranspiration index reconstruction in the Taihe Mountains using tree-ring widths for the last 283 years. *PLoS ONE* **2015**, *10*, e0133605. [CrossRef]
47. CAMS (Chinese Academy of Meteorological Science). *Yearly Charts of Dryness/Wetness in China for the Last 500-Year Period*; China Cartographic Publishing House: Beijing, China, 1981. (In Chinese)

48. Zhang, D.E.; Li, X.Q.; Liang, Y.Y. Continued complement (1993–2000) of yearly charts of dryness/wetness in China for the last 500-year period. *J. Appl. Meteorol. Sci.* **2003**, *14*, 379–384. (In Chinese) [CrossRef]
49. Zhang, D.E.; Liu, C.Z. Continued complement (1980–1992) of yearly charts of dryness/wetness in China for the last 500-year period. *Meteor. Mon.* **1993**, *19*, 41–45. (In Chinese)